ORIGINAL ARTICLE

Photobiomodulation therapy inhibits oral submucous fibrosis in mice

Min-Hsuan Chiang[1,2] | Kun-Tsung Lee[1,3] | Chia-Hsin Chen[2,4,5,6,7] | Ker-Kong Chen[1,8] | Yan-Hsiung Wang[1,2,7] (ID)

[1]School of Dentistry, College of Dental Medicine, Kaohsiung Medical University, Kaohsiung, Taiwan

[2]College of Medicine, Orthopaedic Research Center, Kaohsiung Medical University, Kaohsiung, Taiwan

[3]Department of Oral Hygiene, College of Dental Medicine, Kaohsiung Medical University, Kaohsiung, Taiwan

[4]Department of Physical Medicine and Rehabilitation, Kaohsiung Municipal Ta-Tung Hospital, Kaohsiung Medical University, Kaohsiung, Taiwan

[5]Department of Physical Medicine and Rehabilitation, Kaohsiung Medical University Hospital, Kaohsiung Medical University, Kaohsiung, Taiwan

[6]Department of Physical Medicine and Rehabilitation, School of Medicine, College of Medicine, Kaohsiung Medical University, Kaohsiung, Taiwan

[7]Regenerative Medicine and Cell Therapy Research Center, Kaohsiung Medical University, Kaohsiung, Taiwan

[8]Department of Dentistry, Kaohsiung Medical University Hospital, Kaohsiung Medical University, Kaohsiung, Taiwan

Correspondence
Yan-Hsiung Wang and Ker-Kong Chen, School of Dentistry, College of Dental Medicine, Kaohsiung Medical University, 100, Shih-Chuan 1st Road, Kaohsiung 80708, Taiwan.
Emails: yhwang@kmu.edu.tw; enamel@kmu.edu.tw

Funding information
Kaohsiung Medical University, Grant/Award Number: KMU-TC108A02-0, KMU-TP104B11, KMU-TP105B11 and KMUH108-8M59; Ministry of Science and Technology, Taiwan, Grant/Award Number: MOST104-2314-B-037-059-MY2

Abstract

Objectives: Oral submucous fibrosis (OSMF) is a chronic inflammatory disease and a potentially malignant oral disorder. However, the best therapeutic treatment for OSMF remains uncertain. Our previous study showed that photobiomodulation (PBM) therapy and forskolin could reduce arecoline-induced fibrosis reactions via the cAMP pathway. The present study aimed to establish an animal model of areca nut extract (ANE)-induced OSMF and to evaluate the therapeutic potential of PBM and forskolin for ANE-induced OSMF.

Subjects and methods: The mice were divided into five groups. The buccal tissues were harvested for histomorphological analysis and immunoblotting.

Results: Our results showed that PBM significantly reduced the development of ANE-induced OSMF, quantified by changes in submucosal layer thickness and collagen deposition. Additionally, PBM could extensively reduce the protein expression of the fibrotic marker genes alpha-smooth muscle actin (α-SMA) and connective tissue growth factor (CTGF) in buccal submucous lesions. However, forskolin treatment significantly decreased the protein expression of fibrotic marker genes but slightly decreased the observed histomorphological changes.

Conclusions: We established an ANE-induced OSMF mouse model, which also provided a model for the development of a therapeutic treatment for OSMF. The antifibrotic effects of PBM and forskolin may be useful for clinical interventions.

1 | INTRODUCTION

Oral submucous fibrosis (OSMF) was first reported in the mid-20th century and was found in the oral cavity, with symptoms of idiopathic partial epithelial atrophy and sclerosis (Ali, Patil, Patil, & Prasant, 2014). OSMF is a potentially malignant oral disorder with a high risk of malignant transformation. Several studies have indicated that 7%–30% of OSMF patients may experience transformation into oral squamous cell carcinoma (OSCC), particularly among people of Asian descent, with high prevalence in the Indian subcontinent and South-East Asia (Awadallah, Idle, Patel, & Kademani, 2018; Mello et al., 2018; Wollina, Verma, Ali, & Patil, 2015). Approximately 3–16 years after a patient is first diagnosed with OSMF, oral cancer may develop (Awadallah et al., 2018). From a survey conducted decades ago, it was estimated that 2.5 million people were affected by OSMF worldwide, and the number of patients has increased tremendously over time (Mello et al., 2018; Tsai, Ma, & Shieh, 1999).

Common clinical features of OSMF include excessive salivation or xerostomia, burning sensation, altered sensory perception, impaired oral activity, and eventual inability to open the mouth (More & Rao, 2019). Because it affects the oral cavity, including the buccal mucosa, the mucous membranes of the lips, the cushion after the molars, the soft palate, and the base of the mouth, changes in the elasticity of the fibers occur (Warnakulasuriya, 2018). The disease is characterized by neutrophil and eosinophil infiltration of proximal epithelial cells, followed by progressive fibrosis and scar formation in the lamina propria and submucosa, resulting in hardening of the oral mucosa and trismus (Ali et al., 2014). As previously mentioned, fibrotic changes can also be detected in the pharynx, esophagus, and accessory lip muscles of the eustachian tube in rare cases (Wollina et al., 2015).

The pathogenesis of OSMF is multifactorial. Although many etiological factors have been identified for this disease, various epidemiological and histopathological studies on fibroblasts and keratinocytes have demonstrated that betel chewing is the most consistent and significant risk factor for OSMF (Ali et al., 2014; Khan, Chatra, Prashanth, Veena, & Rao, 2012). Many physiological and biochemical pathways have been suggested to be associated with the above-mentioned processes leading to OSMF. Many in vitro studies indicate that areca nut extract (ANE) enhances collagen formation by transdifferentiating myofibroblasts that express the intracellular marker protein α-SMA and further reduces collagen degradation by regulating the activity of matrix metalloproteinases (MMPs) (Dai et al., 2014; Gadbail et al., 2018; Tilakaratne, Klinikowski, Saku, Peters, & Warnakulasuriya, 2006). Furthermore, ANE induces fibrosis through signal transduction pathways associated with transforming growth factor-beta (TGF-beta) (Khan, Kumar, Pant, Narra, & Kondaiah, 2012), CTGF (Yeh et al., 2017), interleukin 6 (IL-6), and

prostaglandin E2 (PGE2) (Chang et al., 2004) in different cell lines. However, the exact molecular mechanism underlying the carcinogenicity of OSMF induced by betel chewing remains to be clarified; most of the relevant information is limited to clinical observations and in vitro studies (Chang et al., 2014; Ma, Tsai, & Shieh, 1995; Maher, Lee, Warnakulasuriya, Lewis, & Johnson, 1994).

Recently, we successfully established a mouse model of localized dermal fibrosis that mimics the pathologic development of OSMF within 4 weeks after subcutaneous injection of ANE in the backs of the mice (Chiang et al., 2016). In addition, our previous study found that photobiomodulation (PBM) and forskolin could reduce arecoline-induced fibrosis via the cAMP pathway (Yeh et al., 2017). PBM has also been shown to modulate the inflammatory response and ameliorate different fibrotic diseases, as indicated by reduced formation of scar tissue after myocardial infarction in rats and dogs (Oron et al., 2001), decreased renal interstitial fibrosis (Oliveira et al., 2012), and muscle regeneration and prevention of fibrosis in the rat tibialis anterior muscle after cryolesion formation (Assis et al., 2013). The therapeutic effect of PBM on OSMF is largely unknown. Therefore, we established an ANE-induced OSMF model and further analyzed the effects of PBM and forskolin treatment on OSMF.

2 | MATERIALS AND METHODS

2.1 | Chemicals and reagents

ANE was purchased from Haw Yaun Vacuum Biochemical Technology Co., Ltd. (Taoyuan). Anti-CTGF, anti-α-SMA, anti-beta actin, and horseradish peroxidase-conjugated secondary antibodies were purchased from Cell Signaling Technology (Danvers, MA). General chemicals used in this study were purchased from Sigma unless indicated otherwise.

2.2 | PBM treatment

The laser treatment was similar to that described in our previous study (Wang et al., 2018). A continuous-wave (CW)-mode 660 nm gallium–aluminum–arsenide (GaAlAs) laser was purchased from Transverse Industries (Taipei, Taiwan). Laser treatment was carried out with a distance of 5 mm between the laser source and the buccal lesion. The maximum power of the laser was 70 mW, and the distance between the laser source and the bottom of the plate could be adjusted to match the intended target size. The power density was 15.17 mW*cm^2, and an exposure irradiation energy of 8 J*cm^2 was applied to mouse buccal lesions once a day, five times a week.

2.3 | Animals

All animal experiments were approved (number 103,149) by the Institutional Animal Care and Use Committee (IACUC) of Kaohsiung Medical University. Six-week-old male BALB/c mice were obtained from LASCO (BioLASCO Co. Ltd., Taipei). Mice were acclimated for one week in a standard animal housing facility before the experiments.

All mice were randomly divided into five groups: 1) PBS (n = 12); 2) BLM (n = 12); 3) ANE (n = 12); 4) ANE + PBM (n = 5); and 5) ANE + forskolin (n = 5). The mice were sub-buccally injected with PBS, bleomycin (0.5 mg/ml), and ANE (20 mg/ml) every two days. Bleomycin-treated mice were used as a positive control for fibrosis. For the ANE + PBM treatment, the mice were sub-buccally injected with ANE and subjected to 8 J/cm^2 PBM treatment. For the ANE + forskolin treatment, the mice were sub-buccally injected with ANE and intraperitoneally (IP) injected with 10 mg/ml forskolin 5 days a week. All animals were sacrificed one month after the treatments. The buccal tissues were harvested, and each tissue was divided into 2 parts for histological analysis and immunoblotting.

2.4 | Hematoxylin and eosin (H&E) staining

Tissue samples were obtained from the sacrificed animals and fixed in 10% formalin. Following fixation, the tissues were dehydrated and embedded in paraffin wax according to standard procedures. Serial 5-μm sections were obtained and routinely stained with H&E. Hematoxylin in complex with aluminum salts is cationic and acts as a basic dye to stain nucleic acids in the nucleus blue. Full cellular details were obtained by counterstaining with the eosin mixture. Eosin is anionic and acts as an acidic dye to stain acidophilic components in the tissue pink. Images captured under light microscopy were analyzed using Image-Pro Plus software version 5.0.

2.5 | Masson's trichrome stain

After deparaffinization, the tissue sections were stained with the acid dye Biebrich scarlet for 5 min. The dye binds with acidophilic tissue components, that is, the cytoplasm and muscle fibers. After two washes with PBS, the section was then treated with phosphotungstic/phosphomolybdic acid for 10 min. The phospho-acids cause the Biebrich scarlet to diffuse out of the collagen, while the less permeable components retain the red color. The basic molecular sites of collagenic molecules were later bound with aniline blue and stained blue. Images captured under light microscopy were analyzed using Image-Pro Plus software version 5.0 to observe the deposition of collagen.

2.6 | Western blot analysis

Tissues of the buccal mucosa were isolated from the mice. To detect individual protein expression, protein was extracted from the mouse sample tissues using RIPA lysis buffer (Sigma-Aldrich, Germany). After the removal of the tissue debris by centrifugation, the concentration of the protein in the supernatant was measured using the BCA Protein Assay Kit (Thermo Scientific, Waltham, MA, USA.). Forty micrograms of protein lysate from each mouse was fractionated by 10% SDS-PAGE and transferred to a PVDF membrane. Non-specific reactivity was blocked in 5% non-fat dry milk in PBST [10 mmol/L Tris-HCl (pH 7.5), 150 mmol/L NaCl, and 0.05% Tween-20] for 1 hr at 37°C. The membranes were blotted with primary antibodies specific for each protein, with dilutions made according to the manufacturer's recommendations. After incubation, the membranes were washed 3 times in PBST for 10 min and subsequently incubated with the appropriate secondary antibodies (Sigma-Aldrich, Germany), followed by development with Western Lightning^{TM} Chemiluminescence Reagent *Plus* (Perkin Elmer, Waltham, MA, USA), and chemiluminescence signals were detected and captured using an AutoChemi^{TM} Image and Analysis System (UVP, Upland, CA, USA).

2.7 | Statistical analysis

All data are presented as the mean ± *SD*, and data analysis was performed by using SPSS version 17.0. Statistically significant differences were determined by analysis of variance (ANOVA) followed by Tukey's *post hoc* test for multiple comparisons. The results are shown as the mean ± *SD*. The levels of statistical significance are as follows: *p < .05, **p < .01, and ***p < .01 relative to the PBS control group; #p < .05, ##p < .01, and ###p < .01 relative to the ANE group.

3 | RESULTS

3.1 | Oral submucosal injection of ANE increased the buccal submucosal thickness

We modified our previous ANE-induced dermal fibrosis model to investigate whether oral submucosal injection of ANE could induce OSMF (Chiang et al., 2016). Mice were treated with ANE, and the morphologic changes were analyzed on days 14 and 30 (Figure 1a, b). The morphological changes of the oral buccal submucosa were analyzed by H&E staining and are shown in Figure 1a. After bleomycin (BLM) and ANE treatment, the lamina propria thickness was increased compared with that in the PBS control group. The ANE treatment groups showed a time-dependent increase in lamina propria thickness (Figure 1c). However, the BLM treatment group did not exhibit thickening of the lamina propria over time.

3.2 | Subcutaneous injection of ANE-induced collagen deposition

Collagen deposition is a major characteristic of tissue fibrosis. Next, we further analyzed collagen deposition by Masson's trichrome

FIGURE 1 Histopathological evaluation of the lamina propria and submucosal layer thickness by H&E staining. (a) The injection sites were examined on day 14. The sections were viewed under a microscope at 100× and 400× magnification. Magnified tissue regions are marked by yellow rectangles. (b) The injection sites were examined on day 30. The sections were viewed under a microscope at 100× and 400× magnification. Magnified tissue regions are marked by yellow rectangles. (c) Quantification of the average lamina propria and submucosal layer thickness of the tissue using Image-Pro software. The results are expressed as the mean ± *SD*. **p < .01 relative to the PBS control group
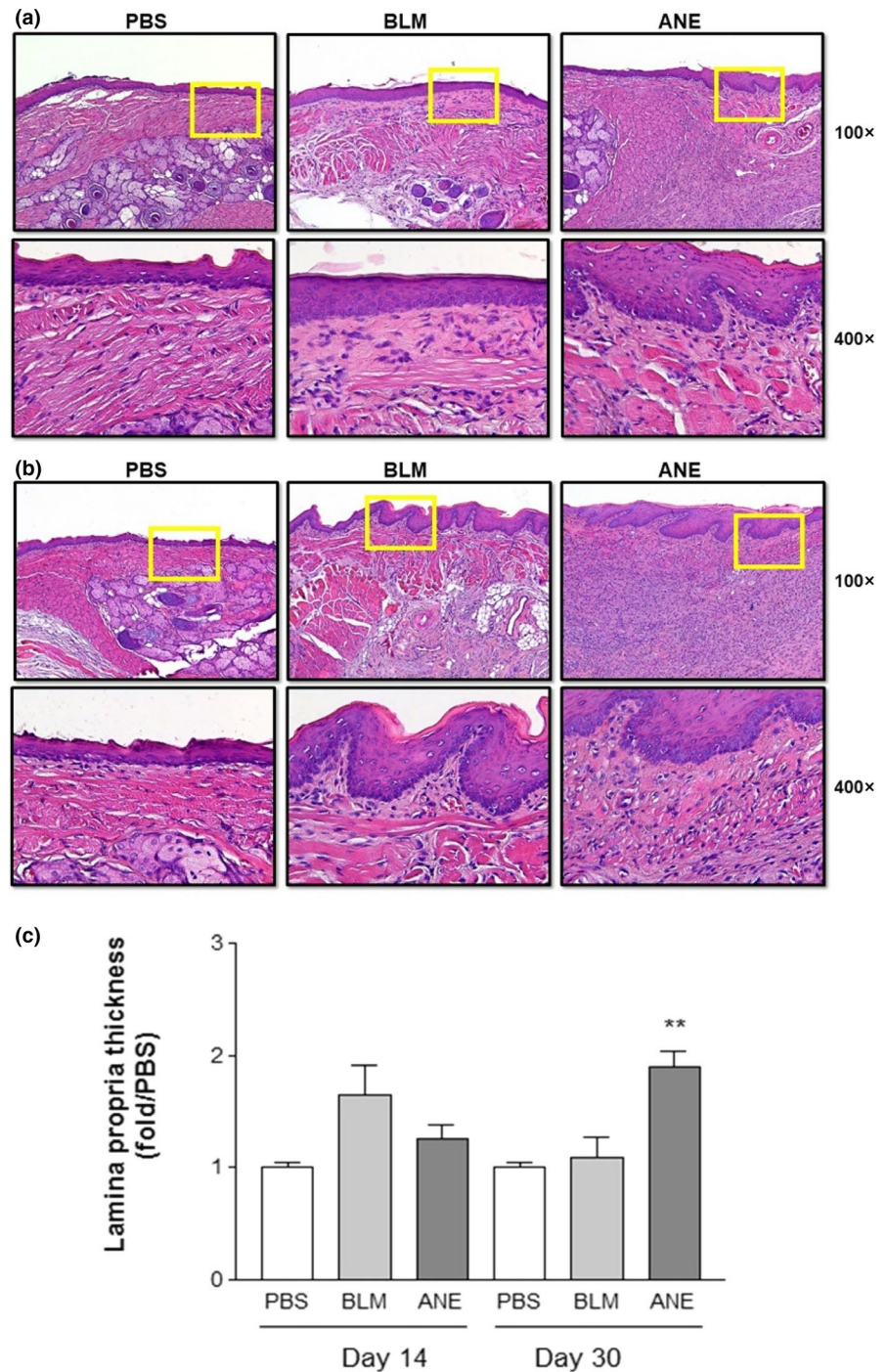
staining. The collagen fibers were stained blue (Figure 2a). After quantifying collagen expression, both the ANE and BLM groups showed significantly stronger collagen staining than the PBS control group on days 14 and 30. Additionally, the BLM treatment group showed significantly stronger collagen staining than the PBS control group on day 30 (Figure 2b). Collagen deposition did not change in the PBS control group at different time points. However, the BLM and ANE treatment groups showed a time-dependent increase in collagen deposition (Figure 2b).

3.3 | The therapeutic effects of PBM and forskolin on ANE-induced buccal submucous fibrosis

Our previous study showed that PBM may activate cAMP signaling and reduce fibrotic gene expression in arecoline-treated cells (Yeh et al., 2017). We further investigated whether PBM and forskolin, an adenylate cyclase activator, could reduce ANE-induced buccal submucous fibrosis in vivo. Mice with ANE-induced buccal submucous fibrosis were cotreated with PBM or forskolin, and morphologic
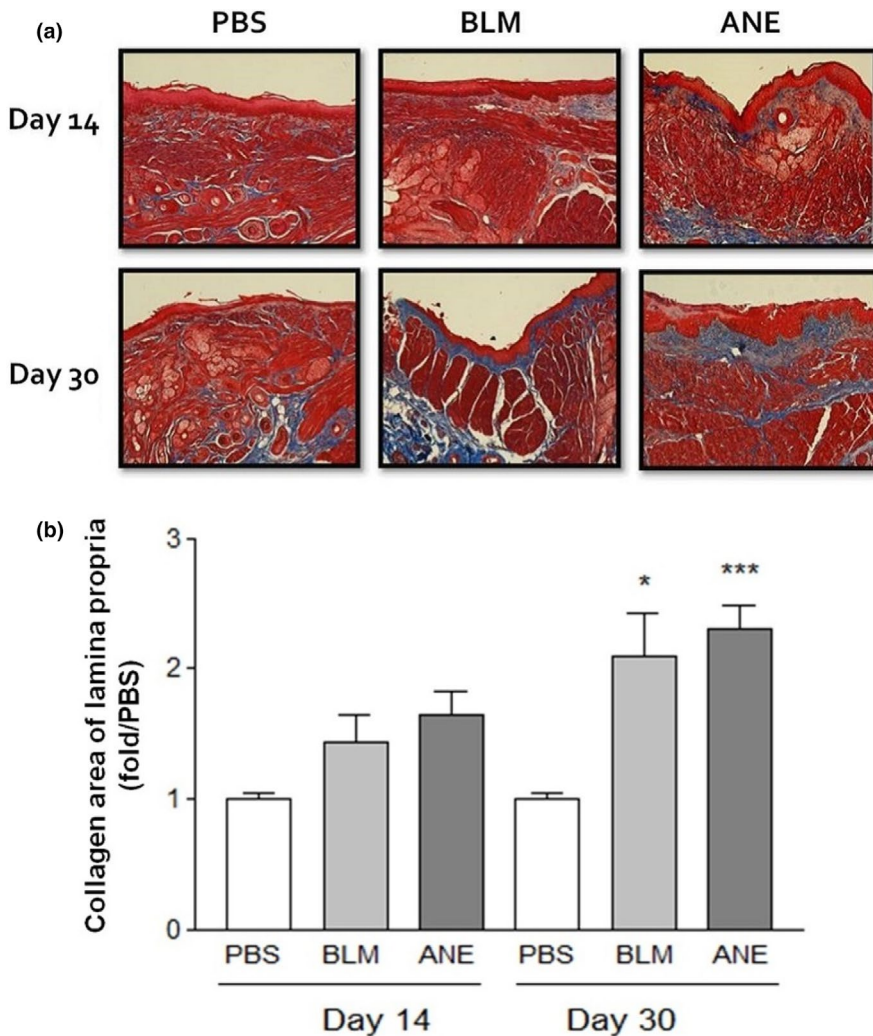
FIGURE 2 Histopathological evaluation of collagen deposition in the lamina propria layer by Masson's trichrome staining. (a) The buccal injection sites were examined on days 14 and 30. The sections were viewed under a microscope at 100× magnification. (b) The intensity of the blue color representing the collagen density was measured using Image-Pro software. The results are expressed as the mean ± *SD*. *p < .05 relative to the PBS control group. ***p < .001 relative to the PBS control group

changes were analyzed by H&E and Masson's trichrome staining. The data showed that ANE led to tissue fibrosis after injection of ANE for 30 days. In the PBM cotreatment group, the histomorphological results showed that PBM could significantly reduce the pathological thickness (Figure 3a, b). Additionally, PBM significantly reduced ANE-induced collagen disposition in the buccal tissue (Figure 3c, d). On the other hand, in the forskolin treatment group, forskolin slightly reduced the effect of ANE-induced buccal submucous fibrosis on both pathological thickness and collagen disposition (Figure 3).

3.4 | PBM and forskolin reduced ANE-induced fibrotic growth factor expression

Next, the expression of fibrotic growth factors was further confirmed by Western blot. A weak staining signal of CTGF and α-SMA was observed in the PBS control group (Figure 4a). Compared with that in the PBS control group, ANE-induced CTGF expression was significantly increased. Consistently, similar α-SMA expression patterns were observed. Additionally, we observed that PBM and

forskolin can effectively reduce the expression of the ANE-induced fibrotic genes CTGF (Figure 4b) and α-SMA (Figure 4c).

4 | DISCUSSION

In our previous study, we showed that subcutaneous injection of ANE can induce dermal fibrosis within one month (Chiang et al., 2016). In this study, we found that injection of ANE into buccal tissues also induced fibrosis within one month, and pathological features similar to those of OSMF were observed. Furthermore, cotreatment of mice with ANE-induced OSMF with PBM or forskolin resulted in less fibrotic tissue. In particular, PBM treatment significantly decreased the expression of fibrotic markers.

Some OSMF animal models have been reported. Sumeth Perera and coworkers established a mouse model that requires 300–600 days for OSMF development (Sumeth Perera et al., 2007). In our present study, we developed an ANE-induced OSMF animal model within one month by buccal mucosa injection. However, Maria, Kamath, Satelur, and Rajkumar (2016) injected areca nut and
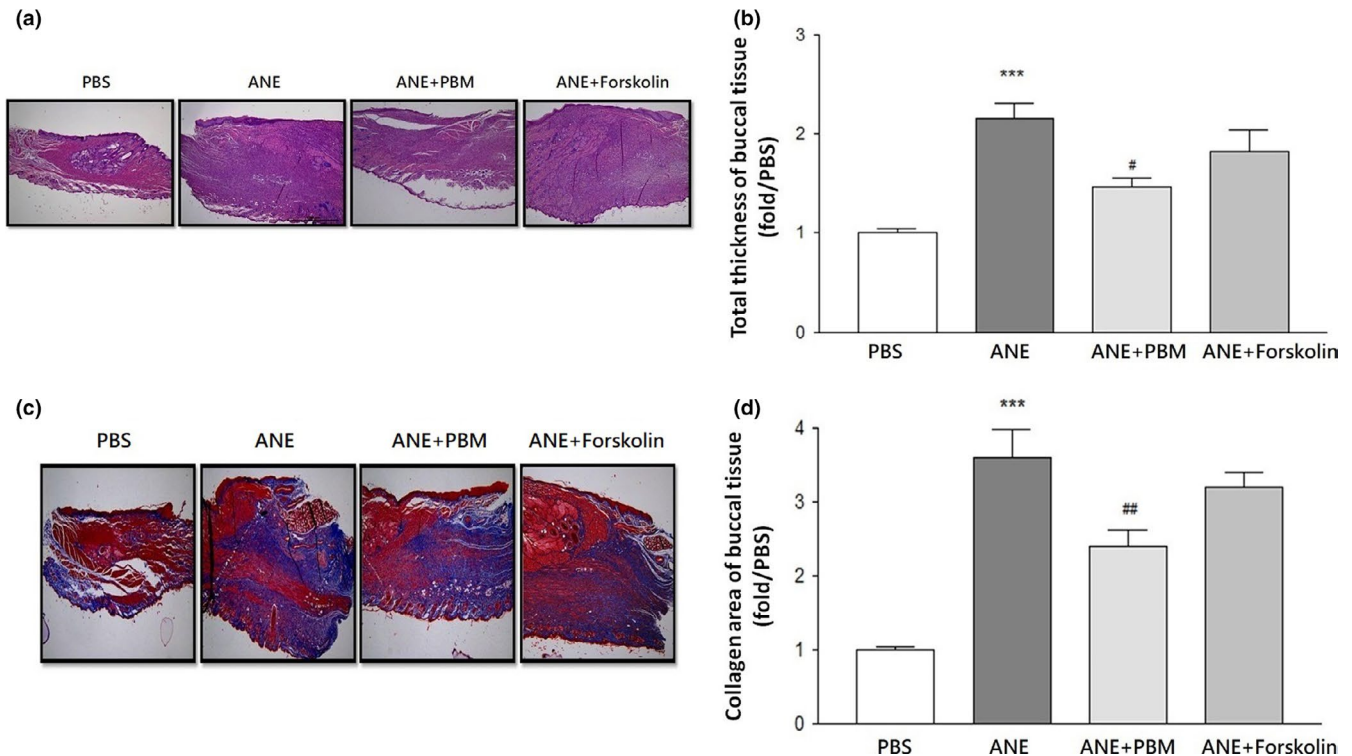
FIGURE 3 Therapeutic effect of PBM and forskolin in ANE-induced buccal submucous fibrosis. (a) The injection sites were examined by H&E staining on day 30. The sections were viewed under a microscope at 100× magnification. (b) Quantification of the average lamina propria and submucosal layer thickness of the tissue using Image-Pro software. (c) The buccal injection sites were examined on day 30 by Masson's trichrome staining. The sections were viewed under a microscope at 40× magnification. (d) The intensity of the blue color representing collagen deposition was measured using Image-Pro software. The results are expressed as the mean ± *SD*. ***$p < .001$ compared with the PBS control group, #$p < .05$ compared with the ANE group, ##$p < .01$ compared with the ANE group

pan masala solutions into the buccal mucosa in rats, and OSMF was observed over a period of 48 weeks. The different time periods for OSMF development may be due to differences in ANE preparation. Maria *et al*. prepared the samples by centrifugation at 15,000 rpm for 30 min. Then, only the supernatant was collected and applied to the animals. In our study, the ANE solution was passed through a 0.22-μm filter to remove bacteria and particles before injection. The ANE content and concentration may be very different between the two studies. We think the solution of chewed betel nut would be similar to the filtered ANE solution but not the centrifuged clear supernatant of the ANE solution. In addition, we found that bleomycin can induce fibrosis in the oral submucosa, which is consistent with the findings of a recent study showing that injection of bleomycin into the buccal mucosa caused pathologic changes similar to those observed in OSMF (Zhang et al., 2016). However, because bleomycin is not an ingredient in natural food, bleomycin-induced OSF is not easy to implicate in the clinical process of OSMF. Recently, Wen *et al*. fed mice with high doses of arecoline (1,000 mg/L) in the drinking water and found OSMF pathologic changes in the oral cavity (Wen et al., 2017). ANE-induced OSMF is a better model to represent the real oral environment to which the buccal tissue is exposed in the chewers. In addition, this approach may not be suitable for the development of OSMF therapeutic methods because the location of OSMF is not easy to predict in the oral cavity.

Patients with OSMF do not have a life-threatening condition, but the symptoms of OSMF, such as trismus, burning pain in the mouth, and malignant transformation, may affect the patient's quality of life. To date, no treatment has been reported to achieve radical cure of OSMF. There are different treatments to relieve the symptoms of OSMF: surgery, physical therapy, and medical treatment. Surgical treatment includes cutting the fibrotic band to release the mucosal trismus, physical therapy includes rehabilitation of oral function by a hot compress or mouth-opening exercises, and medical treatment includes pain relief or inflammatory treatment. In this study, we provide a new animal model of ANE-induced OSMF and show that PBM is a potential therapeutic method for OSMF using this mouse model. However, different biological effects of PBM have been known for several decades. The optical treatment and cellular mechanism remain unclear and controversial. This is because the biological effects of PBM are influenced by many factors, such as wavelength, energy density, and cell/tissue type. For example, the TGF-β signaling pathway plays important roles in both wound healing and tissue fibrosis (Dang et al., 2011; Fekrazad et al., 2018). PBM has been shown to stimulate the TGF-β pathway to enhance cell proliferation and wound healing. However, PBM has also been reported to reduce fibrosis via downregulation of the TGF-β pathway (Ahrabi et al., 2020; Oliveira et al., 2012). The explanation may be that PBM activates different signaling pathways at the same time, and the
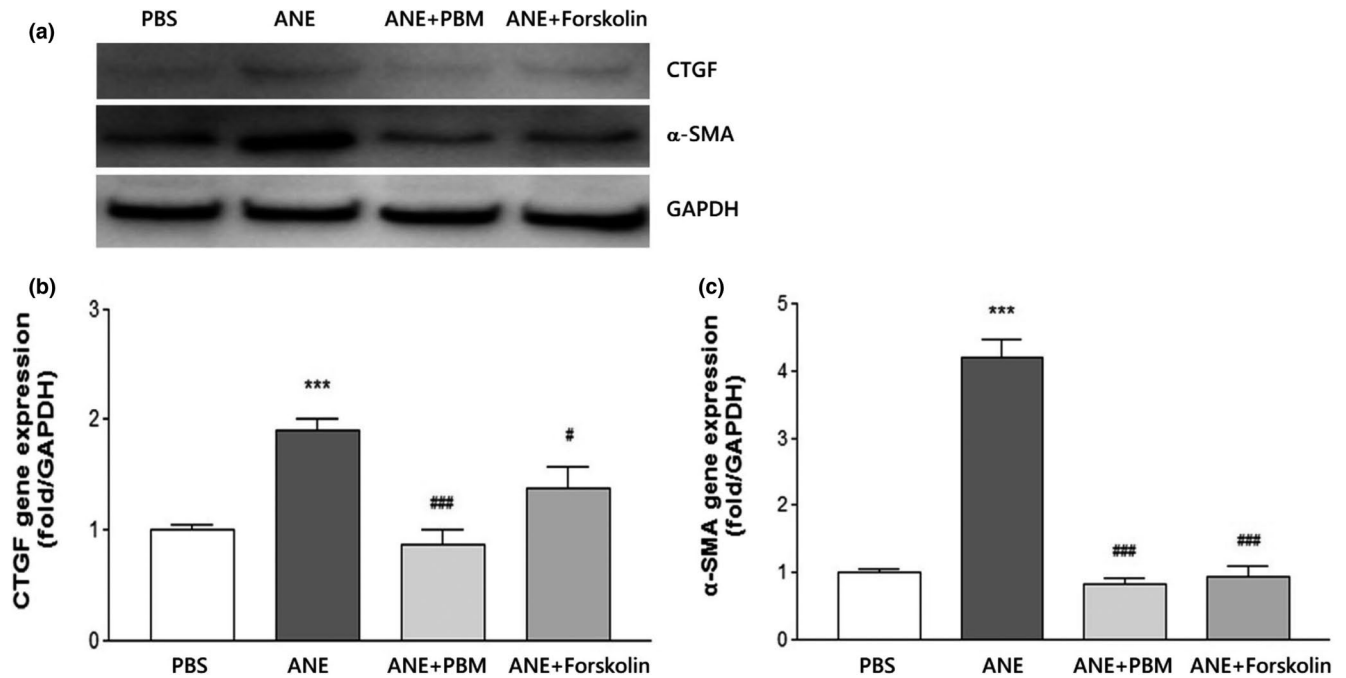
FIGURE 4 PBM and forskolin reduced ANE-induced fibrotic growth factor expression. (a) The expression levels of the fibrotic markers CTGF and α-SMA were detected at the indicated time points by immunoblotting. GAPDH was used as a loading control. (b) CTGF and (c) α-SMA expression were measured using Image-Pro software. The results are expressed as the mean ± *SD*. ***p < .001 compared with the PBS control group, #p < .05 compared with the ANE group, ###p < .001 compared with the ANE group

cross talk among these pathways is complex. Then, PBM moderates the TGF-β pathway to balance the biological effects between wound healing and fibrosis. More studies are necessary to probe the mechanism of PBM in regulating cellular signaling cross talk in different physiological and pathological conditions.

In recent years, it has been found that PBM has a biostimulatory effect on different physiological reactions, including improvement of local blood circulation, regulation of immune responses, and stimulation of cell metabolism and proliferation. Additionally, PBM has been applied in anti-inflammatory treatment and pain relief and promotes wound healing and other therapeutic effects (Chaves, Araujo, Piancastelli, & Pinotti, 2014; Wickenheisser et al., 2019). The role of PBM in fibrotic diseases has also begun to be explored in vitro and in vivo. Our previous experiment demonstrated that PBM could inhibit the expression of arecoline-mediated fibrotic marker genes via cAMP signaling in vitro (Yeh et al., 2017). Sassoli et al. (2016) showed that PBM inhibited the TGF-β1/Smad3-mediated fibroblast–myofibroblast transition. Additionally, PBM has been reported to reduce collagen deposition in rat tendons after trauma (Fillipin et al., 2005), carbon tetrachloride-induced liver cirrhosis (Oliveira-Junior et al., 2013), and renal interstitial fibrosis (Oliveira et al., 2012). According to our previous in vitro study, we showed that PBM could significantly reduce the pathological thickness in ANE-induced OSMF. However, activation of cAMP signaling by forskolin only slightly reduced the pathological thickness in ANE-induced OSMF (Figure 3). The proteins were extracted from only the buccal mucosa for the Western blot analysis, in contrast to the analysis of pathological thickness. The protein

expression levels of CTGF and α-SMA were significantly reduced by PBM and forskolin (Figure 4). The inconsistent results for pathological thickness and protein expression may be due to the use of different tissues in these two assays. These results indicated that the cAMP signaling pathway is not the only pathway that affects the pathological changes and anti-fibrotic effect of PBM in vivo. The detailed mechanism of PBM's anti-fibrotic effect on ANE-induced OSMF should be further investigated.

Although our data showed that OSMF was induced by sub-buccal injection of ANE within one month and that cotreatment with PBM and forskolin could reduce the development of OSMF, the current study has some limitations. First, we did not fully compare the pathological symptoms between clinical samples and the animal model. Therefore, clinical application of the data from this animal model should proceed with caution. Second, OSMF was induced in the mice by ANE, and the mice were cotreated with PBM or forskolin. Thus, our data indicated that PBM and forskolin could reduce the development of OSMF. The interpretation of the therapeutic effect of PBM and forskolin on OSMF requires further investigation.

In summary, we established a stable and rapid-induction ANE-induced OSMF mouse model. We found that PBM reduced the development of fibrosis, quantified by changes in the submucosal layer and lamina propria thickness at the ANE injection sites. Further investigations are underway to study the mechanisms underlying the inhibitory effect of PBM on ANE-induced OSMF. This model not only improves our understanding of ANE-induced fibrosis but also provides a model for the development of therapeutic treatments for OSMF.

AUTHOR CONTRIBUTION

Min-Hsuan Chiang: Formal analysis; Investigation; Methodology; Validation; Writing-original draft. **Kun-Tsung Denzel Lee:** Conceptualization; Validation; Visualization. **Chia-Hsin Chen:** Conceptualization; Resources; Visualization. **Ker-Kong Chen:** Conceptualization; Funding acquisition; Supervision; Visualization; Writing-review & editing. **Yan-Hsiung Wang:** Conceptualization; Funding acquisition; Project administration; Resources; Supervision; Validation; Visualization; Writing-review & editing.

ORCID

Yan-Hsiung Wang ID https://orcid.org/0000-0001-8161-7472

REFERENCES

Ahrabi, B., Bahrami, M., Moghadasali, R., Zamanian-Azodi, M., Khoramgah, M. S., Tabatabaei Mirakabad, F. S., ... Abbaszadeh, H. A. (2020). The effect of low-power laser therapy on the TGF/beta signaling pathway in chronic kidney disease: A review. *Journal of Lasers in Medical Sciences*, 11(2), 220–225. https://doi.org/10.34172/jlms.2020.36

Ali, F. M., Patil, A., Patil, K., & Prasant, M. C. (2014). Oral submucous fibrosis and its dermatological relation. *Indian Dermatology Online Journal*, 5(3), 260–265. https://doi.org/10.4103/2229-5178.137772

Assis, L., Moretti, A. I., Abrahao, T. B., de Souza, H. P., Hamblin, M. R., & Parizotto, N. A. (2013). Low-level laser therapy (808 nm) contributes to muscle regeneration and prevents fibrosis in rat tibialis anterior muscle after cryolesion. *Lasers in Medical Science*, 28(3), 947–955. https://doi.org/10.1007/s10103-012-1183-3

Awadallah, M., Idle, M., Patel, K., & Kademani, D. (2018). Management update of potentially premalignant oral epithelial lesions. *Oral Surgery, Oral Medicine, Oral Pathology and Oral Radiology*, 125(6), 628–636. https://doi.org/10.1016/j.oooo.2018.03.010

Chang, M. C., Wu, H. L., Lee, J. J., Lee, P. H., Chang, H. H., Hahn, L. J., ... Jeng, J. H. (2004). The induction of prostaglandin E2 production, interleukin-6 production, cell cycle arrest, and cytotoxicity in primary oral keratinocytes and KB cancer cells by areca nut ingredients is differentially regulated by MEK/ERK activation. *Journal of Biological Chemistry*, 279(49), 50676–50683. https://doi.org/10.1074/jbc.M404465200

Chang, Y. C., Tsai, C. H., Lai, Y. L., Yu, C. C., Chi, W. Y., Li, J. J., & Chang, W. W. (2014). Arecoline-induced myofibroblast transdifferentiation from human buccal mucosal fibroblasts is mediated by ZEB1. *Journal of Cellular and Molecular Medicine*, 18(4), 698–708. https://doi.org/10.1111/jcmm.12219

Chaves, M. E., Araujo, A. R., Piancastelli, A. C., & Pinotti, M. (2014). Effects of low-power light therapy on wound healing: LASER x LED. *Anais Brasileiros De Dermatologia*, 89(4), 616–623. https://doi.org/10.1590/abd1806-4841.20142519

Chiang, M. H., Chen, P. H., Chen, Y. K., Chen, C. H., Ho, M. L., & Wang, Y. H. (2016). Characterization of a novel dermal fibrosis model induced by areca nut extract that mimics oral submucous fibrosis. *PLoS ONE*, 11(11), e0166454. https://doi.org/10.1371/journal.pone.0166454

Dai, J. P., Chen, X. X., Zhu, D. X., Wan, Q. Y., Chen, C., Wang, G. F., ... Li, K. S. (2014). Panax notoginseng saponins inhibit areca nut extract-induced oral submucous fibrosis in vitro. *Journal of Oral Pathology and Medicine*, 43(6), 464–470. https://doi.org/10.1111/jop.12158

Dang, Y., Liu, B., Liu, L., Ye, X., Bi, X., Zhang, Y., & Gu, J. (2011). The 800-nm diode laser irradiation induces skin collagen synthesis by stimulating TGF-beta/Smad signaling pathway. *Lasers in Medical Science*, 26(6), 837–843. https://doi.org/10.1007/s10103-011-0985-z

Fekrazad, R., Sarrafzadeh, A., Kalhori, K. A. M., Khan, I., Arany, P. R., & Giubellino, A. (2018). Improved wound remodeling correlates with modulated TGF-beta expression in skin diabetic wounds following combined red and infrared photobiomodulation treatments. *Photochemistry and Photobiology*, 94(4), 775–779. https://doi.org/10.1111/php.12914

Fillipin, L. I., Mauriz, J. L., Vedovelli, K., Moreira, A. J., Zettler, C. G., Lech, O., ... González-Gallego, J. (2005). Low-level laser therapy (LLLT) prevents oxidative stress and reduces fibrosis in rat traumatized Achilles tendon. *Lasers in Surgery and Medicine*, 37(4), 293–300. https://doi.org/10.1002/lsm.20225

Gadbail, A. R., Chaudhary, M., Sarode, S. C., Gondivkar, S., Tekade, S. A., Zade, P., ... Patil, S. (2018). Ki67, CD105, and alpha-SMA expression supports the transformation relevant dysplastic features in the atrophic epithelium of oral submucous fibrosis. *PLoS ONE*, 13(7), e0200171. https://doi.org/10.1371/journal.pone.0200171

Khan, I., Kumar, N., Pant, I., Narra, S., & Kondaiah, P. (2012). Activation of TGF-beta pathway by areca nut constituents: A possible cause of oral submucous fibrosis. *PLoS ONE*, 7(12), e51806. https://doi.org/10.1371/journal.pone.0051806

Khan, S., Chatra, L., Prashanth, S. K., Veena, K. M., & Rao, P. K. (2012). Pathogenesis of oral submucous fibrosis. *Journal of Cancer Research & Therapy*, 8(2), 199–203. https://doi.org/10.4103/0973-1482.98970

Ma, R. H., Tsai, C. C., & Shieh, T. Y. (1995). Increased lysyl oxidase activity in fibroblasts cultured from oral submucous fibrosis associated with betel nut chewing in Taiwan. *Journal of Oral Pathology and Medicine*, 24(9), 407–412. https://doi.org/10.1111/j.1600-0714.1995.tb01210.x

Maher, R., Lee, A. J., Warnakulasuriya, K. A., Lewis, J. A., & Johnson, N. W. (1994). Role of areca nut in the causation of oral submucous fibrosis: A case-control study in Pakistan. *Journal of Oral Pathology and Medicine*, 23(2), 65–69. https://doi.org/10.1111/j.1600-0714.1994.tb00258.x

Maria, S., Kamath, V. V., Satelur, K., & Rajkumar, K. (2016). Evaluation of transforming growth factor beta1 gene in oral submucous fibrosis induced in Sprague-Dawley rats by injections of areca nut and pan masala (commercial areca nut product) extracts. *Journal of Cancer Research & Therapy*, 12(1), 379–385. https://doi.org/10.4103/0973-1482.148729

Mello, F. W., Miguel, A. F. P., Dutra, K. L., Porporatti, A. L., Warnakulasuriya, S., Guerra, E. N. S., & Rivero, E. R. C. (2018). Prevalence of oral potentially malignant disorders: A systematic review and meta-analysis. *Journal of Oral Pathology and Medicine*, 47(7), 633–640. https://doi.org/10.1111/jop.12726

More, C. B., & Rao, N. R. (2019). Proposed clinical definition for oral submucous fibrosis. *Journal of Oral Biology and Craniofacial Research*, 9(4), 311–314. https://doi.org/10.1016/j.jobcr.2019.06.016

Oliveira, F. A. M., Moraes, A. C. M., Paiva, A. P., Schinzel, V., Correa-Costa, M., Semedo, P., ... Sanders-Pinheiro, H. (2012). Low-level laser therapy decreases renal interstitial fibrosis. *Photomedicine and Laser Surgery*, 30(12), 705–713. https://doi.org/10.1089/pho.2012.3272

Oliveira-Junior, M. C., Monteiro, A. S., Leal-Junior, E. C., Munin, E., Osorio, R. A., Ribeiro, W., & Vieira, R. P. (2013). Low-level laser therapy ameliorates CCl4-induced liver cirrhosis in rats. *Photochemistry and Photobiology*, *89*(1), 173–178. https://doi.org/10.1111/j.1751-1097.2012.01211.x

Oron, U., Yaakobi, T., Oron, A., Hayam, G., Gepstein, L., Rubin, O., … Haim, S. B. (2001). Attenuation of infarct size in rats and dogs after myocardial infarction by low-energy laser irradiation. *Lasers in Surgery and Medicine*, *28*(3), 204–211. https://doi.org/10.1002/lsm.1039

Sassoli, C., Chellini, F., Squecco, R., Tani, A., Idrizaj, E., Nosi, D., … Zecchi-Orlandini, S. (2016). Low intensity 635 nm diode laser irradiation inhibits fibroblast-myofibroblast transition reducing TRPC1 channel expression/activity: New perspectives for tissue fibrosis treatment. *Lasers in Surgery and Medicine*, *48*(3), 318–332. https://doi.org/10.1002/lsm.22441

Sumeth Perera, M. W., Gunasinghe, D., Perera, P. A., Ranasinghe, A., Amaratunga, P., Warnakulasuriya, S., & Kaluarachchi, K. (2007). Development of an in vivo mouse model to study oral submucous fibrosis. *Journal of Oral Pathology and Medicine*, *36*(5), 273–280. https://doi.org/10.1111/j.1600-0714.2007.00523.x

Tilakaratne, W. M., Klinikowski, M. F., Saku, T., Peters, T. J., & Warnakulasuriya, S. (2006). Oral submucous fibrosis: Review on aetiology and pathogenesis. *Oral Oncology*, *42*(6), 561–568. https://doi.org/10.1016/j.oraloncology.2005.08.005

Tsai, C. C., Ma, R. H., & Shieh, T. Y. (1999). Deficiency in collagen and fibronectin phagocytosis by human buccal mucosa fibroblasts in vitro as a possible mechanism for oral submucous fibrosis. *Journal of Oral Pathology and Medicine*, *28*(2), 59–63. https://doi.org/10.1111/j.1600-0714.1999.tb01997.x

Wang, Y. H., Wu, J. Y., Kong, S. C., Chiang, M. H., Ho, M. L., Yeh, M. L., & Chen, C. H. (2018). Low power laser irradiation and human adipose-derived stem cell treatments promote bone regeneration in critical-sized calvarial defects in rats. *PLoS ONE*, *13*(4), e0195337. https://doi.org/10.1371/journal.pone.0195337

Warnakulasuriya, S. (2018). Clinical features and presentation of oral potentially malignant disorders. *Oral Surgery, Oral Medicine, Oral Pathology and Oral Radiology*, *125*(6), 582–590. https://doi.org/10.1016/j.oooo.2018.03.011

Wen, Q. T., Wang, T., Yu, D. H., Wang, Z. R., Sun, Y., & Liang, C. W. (2017). Development of a mouse model of arecoline-induced oral mucosal fibrosis. *Asian Pacific Journal of Tropical Medicine*, *10*(12), 1177–1184. https://doi.org/10.1016/j.apjtm.2017.10.026

Wickenheisser, V. A., Zywot, E. M., Rabjohns, E. M., Lee, H. H., Lawrence, D. S., & Tarrant, T. K. (2019). Laser light therapy in inflammatory, musculoskeletal, and autoimmune disease. *Current Allergy and Asthma Reports*, *19*(8), 37. https://doi.org/10.1007/s11882-019-0869-z

Wollina, U., Verma, S. B., Ali, F. M., & Patil, K. (2015). Oral submucous fibrosis: An update. *Clinical, Cosmetic and Investigational Dermatology*, *8*, 193–204. https://doi.org/10.2147/CCID.S80576

Yeh, M. C., Chen, K. K., Chiang, M. H., Chen, C. H., Chen, P. H., Lee, H. E., & Wang, Y. H. (2017). Low-power laser irradiation inhibits arecoline-induced fibrosis: An in vitro study. *International Journal of Oral Science*, *9*(1), 38–42. https://doi.org/10.1038/ijos.2016.49

Zhang, S. S., Gong, Z. J., Xiong, W., Wang, X., Min, Q., Luo, C. D., & Ling, T. Y. (2016). A rat model of oral submucous fibrosis induced by bleomycin. *Oral Surgery, Oral Medicine, Oral Pathology and Oral Radiology*, *122*(2), 216–223. https://doi.org/10.1016/j.oooo.2015.07.042